Terahertz and infrared Smith-Purcell radiation from Babinet metasurfaces: Loss and efficiency

Liu Liu, Huiting Chang, Chi Zhang, Yanan Song, and Xinhua Hu*

Department of Materials Science and Key Laboratory of Micro- and Nano-Photonic Structures (Ministry of Education), Fudan University, Shanghai 200433, China

(Received 7 April 2017; revised manuscript received 6 October 2017; published 25 October 2017)

When a charged particle moves close and parallel to the surface of a Babinet metasurface composed of metallic C-aperture resonators, strong electromagnetic radiation arises at resonant frequency. Here we systematically study the Smith-Purcell effects in Babinet metasurfaces with different periods. By tuning the period, the resonant (or working) frequency of the metasurface can vary from GHz to THz and infrared ranges. It is found that for working frequencies lower than 10 GHz, the ratio of absorption loss to input power is about 3.7%. Although the loss ratio increases with increasing working frequency, it remains as low as 11% (29%) at a working frequency of 10 THz (224 THz). Due to the existence of loss, a nonlinear relationship is also found between resonant frequency and the reciprocal of period. Our results suggest that Babinet metasurfaces could be a good candidate for fabricating efficient, compact THz and infrared free-electron light sources.

DOI: 10.1103/PhysRevB.96.165435

I. INTRODUCTION

Far-field radiation of light can be produced when a charged particle moves close and parallel to the surface of a one-dimensional (1D) metallic grating. This phenomenon, first observed by Smith and Purcell in 1953 [1], is an important extension of Cherenkov effect and forms the basis of many applications such as particle detectors and radiation generators [2–4].

Metasurfaces are two-dimensional metamaterials composed of subwavelength building blocks or meta-atoms [5]. By carefully designing the structure and arrangement of meta-atoms, metasurfaces allow us to attain numerous novel optical phenomena and devices [6–18]. Recently, it has been demonstrated that cross-polarized Smith-Purcell radiation can be generated from Babinet metasurfaces consisting of metallic C-aperture resonators [19]. The radiation intensity at resonant frequency can be 3.4 times of that in a traditional 1D metallic grating. By combining the metasurface with a waveguide, strong radiations have further been observed in the GHz regime [20]. These studies present a new route to control the amplitude and polarization of Smith-Purcell emissions [19,20], which greatly enriches the context of Cherenkov effects in complex artificial structures [21–33].

Reducing energy consumption and improving energy efficiency are important issues for human beings in modern society. For the Smith-Purcell effects in Babinet metasurfaces [19], the energy of swift charged particles can be converted not only into useful radiations but also into unwanted heat in the metal. However, such Ohmic loss (or absorption loss) has seldom been discussed in previous work [19]. It remains unknown whether a low absorption loss can be achieved especially when Babinet metasurfaces work at high frequencies (such as THz and infrared ranges [34]).

In this paper we investigate the Smith-Purcell effects in Babinet metasurfaces with different periods. By tuning the period, the resonant (or working) frequency can vary from GHz to THz and infrared ranges. It is found that the ratio of absorption loss to input power is 3.7% at a working frequency of 10 GHz. Although the loss ratio increases with increasing the working frequency, it remains as low as 11% (29%) at a working frequency of 10 THz (224 THz). For higher working frequencies, an upper limit of about 33% is uncovered for the loss ratio.

II. METHODS

The Babinet metasurface under study is a metallic slab perforated with a square lattice of C apertures, as shown in Fig. 1(a). The metasurface has a period of p in both x and y directions, and a thickness of h in the z direction. The C apertures, which are directed to the x direction, have an outer (inner) radius of r_1 (r_2) and a central angle of $2\pi - \alpha$. Assume the metasurface is in vacuum and its upper surface is located at $z = 0$. A uniform sheet of charged particles, which is in the x-y plane at $z = z_0$, moves with a velocity of v along the x direction. The current density can be expressed as $\bar{J}(x,z,t) = \hat{x} q v \delta(z - z_0)\delta(x - vt) = \int d\omega \bar{J}(x,z,\omega) e^{-i\omega t}$. Here q is the charge per unit length in the y direction. After Fourier transform, the current density in the frequency domain can be given by

$$\bar{J}(x,z,\omega) = \hat{x} I_0 \delta(z - z_0) e^{i k_x x}, \tag{1}$$

where $k_x = \omega/v$, $I_0 = q/(2\pi)$, and ω is the angular frequency. Such a current source can generate an evanescent field in the region with $0 < z < z_0$, namely

$$\bar{H}_i = \hat{y} H_{iy}, \quad \bar{E}_i = -(\hat{x} i\gamma + \hat{z} k_x) Z_0 H_{iy}/k_0. \tag{2}$$

Here $H_{iy} = (I_0/2) e^{i k_x x + \gamma (z - z_0)}$, $\gamma = \sqrt{k_x^2 - k_0^2}$, $k_0 = \omega/c$ is the vacuum wave number, c is the light velocity in vacuum, and $Z_0 = 376.7\,\Omega$ is the vacuum impedance.

When the metasurface is illuminated by the evanescent field described by Eq. (2), reflected fields can be generated above the metasurface and they can be expressed in terms of Floquet modes as

$$\bar{H}_r = \sum_{m,n} \bar{H}_{rmn} e^{i k_{xmn} x + i k_{ymn} y + i k_{zmn} z}. \tag{3}$$

*huxh@fudan.edu.cn

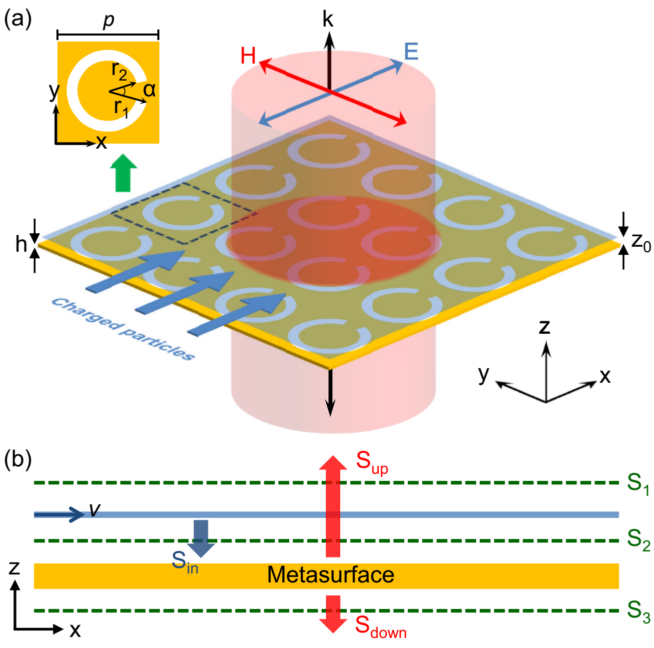

FIG. 1. Schematic of the Smith-Purcell emission from a Babinet metasurface. The Babinet metasurface is a metallic slab perforated by a square lattice of C apertures. The metasurface is in the x-y plane and has a thickness h and period p. (a) A uniform sheet of charged particles, which is parallel and close to the metasurface, moves with a velocity v along the x direction. The Babinet metasurface generates electromagnetic radiations with frequency $f = v/p$ propagating along the z direction. (b) Side view of (a). S_{in}, S_{up}, S_{down}, and S_{ab} are the input energy flux density, upward emission energy flux density, downward emission energy flux density, and absorption energy flux density, respectively.

Here m and n are integers, $k_{xmn} = k_x + 2m\pi/p$, $k_{ymn} = 2n\pi/p$, and $k_{zmn} = \sqrt{k_0^2 - k_{xmn}^2 - k_{ymn}^2}$ are the wave numbers in the x, y, and z directions, respectively. Similar expressions can also be given for the transmitted fields below the metasurface. Since the Smith-Purcell emissions are propagating in the z direction ($k_{zmn}^2 > 0$), they need to have $n = 0$ (i.e., $k_{ymn} = 0$) and $m < 0$, and their frequencies are given by

$$f = \frac{|m|v}{p\left(1 - \frac{v}{c}\cos\varphi\right)}, \tag{4}$$

where $\varphi = \arccos(k_{xmn}/k_0)$ is the angle between the wave vector of emission and the x direction. In the following, we focus on the fundamental order ($|m| = 1$) of Smith-Purcell emissions in the z direction ($\varphi = \pi/2$), so that Eq. (4) reduces to $f = v/p$.

A commercial finite-element software of COMSOL MULTIPHYSICS was applied to simulate the Babinet metasurfaces [19,35]. A periodic boundary condition with $k_x = 2\pi/p$ was adopted. Figure 1(b) illustrates the details for the simulations of the Smith-Purcell effect. The input energy flux density S_{in}, upward emission energy flux density S_{up}, downward emission energy flux density S_{down}, and absorption energy flux density S_{ab} can be calculated by $S_{\text{in}} = S_1 + S_2$, $S_{\text{up}} = S_1$, $S_{\text{down}} = S_3$, and $S_{\text{ab}} = S_2 - S_3$, respectively. Here S_1, S_2, and S_3 are the z components of Poynting vectors through the three planes near the metasurface [see Fig. 1(b)].

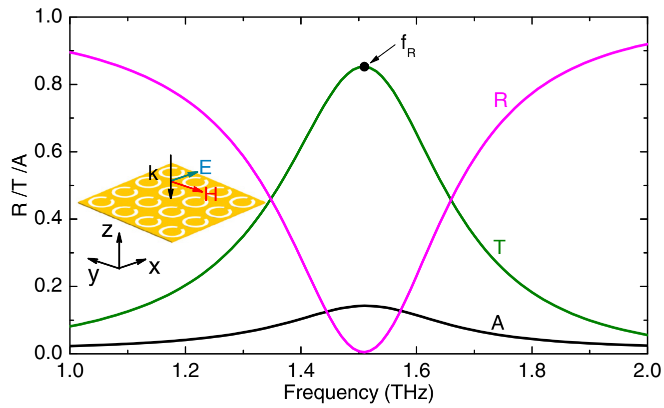

FIG. 2. The simulated reflection (R), transmission (T), and absorption (A) spectra of a Babinet metasurface at normal incidence of propagating waves. The metasurface has parameters of $a = 50\ \mu$m, $h = 200$ nm, $r_1 = 0.4p$, $r_2 = 0.3p$, and $\alpha = 35^\circ$. Both the E field of incident waves and the orientation of C apertures are along the x direction.

III. RESULTS

We consider Babinet metasurfaces with parameters of $r_1 = 0.4p$, $r_2 = 0.3p$, $h = 200$ nm, and $\alpha = 35^\circ$. The metasurfaces are made from a metal (gold) of which the permittivity can be described by a Drude model $\varepsilon_{\text{Au}} = 1 - f_p^2/(f^2 - if v_p)$ with $f_p = 2.174$ PHz and $v_p = 6.48$ THz [36,37]. The swift charged particles are described by Eq. (1) with $I_0 = 1$ A/m, $v = fp$, and $z_0 = p/5$.

A metasurface with a period of $p = 50\ \mu$m is first simulated. Figure 2 shows the simulated reflection (R), transmission (T), and absorption (A) for normal incidence of x-polarized ($E_y = 0$) propagating waves. We can see that a strong resonance occurs at the frequency of 1.51 THz, where the metasurface is nearly transparent ($R = 0$ and $T = 0.86$) and exhibits a small absorption ($A = 0.14$). For frequencies far away from the resonance, the metasurface is almost opaque and highly reflective.

The Smith-Purcell effect is then simulated for the above metasurface [see Fig. 3(a)]. At the resonant frequency, the energy flux densities of S_{in}, S_{up}, S_{down}, and S_{ab} reach their maximums of 14, 6.6, 6.6, and 0.98 W/m^2, respectively. For the upward emission, the E-field amplitude can be obtained as $|E| = \sqrt{2Z_0 S_{\text{up}}} = 70.5$ V/m, agreeing well with the result (70.3 V/m) in [19].

The corresponding emission efficiencies ($S_{\text{up}}/S_{\text{in}}$ and $S_{\text{down}}/S_{\text{in}}$) and loss ratio ($S_{\text{ab}}/S_{\text{in}}$) are also plotted in Fig. 3(b). Unlike the energy flux densities, the emission efficiencies and loss ratio depend weakly on the frequency. At the resonant frequency, both the upward and downward emission efficiencies are 0.47 while the loss ratio is as low as 0.07. We note that when the orientation of C apertures is adjusted from the x direction to the y direction, the energy flux densities of S_{in}, S_{up}, S_{down}, and S_{ab} can be improved by about 26%.

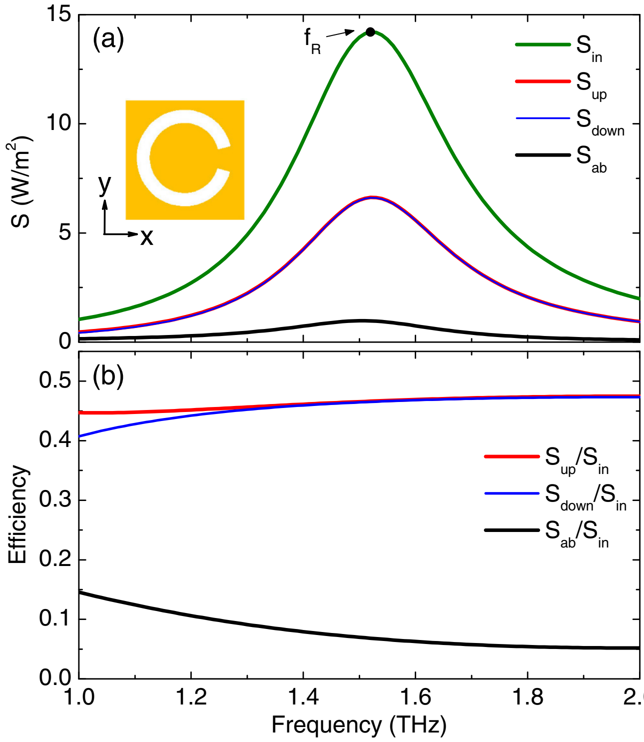

FIG. 3. Characterization of the Smith-Purcell emission from a Babinet metasurface. The metasurface has the same parameters as in Fig. 2. The swift charged particles are described by Eq. (1) with $I_0 = 1$ A/m, $v = pf$, and $z_0 = p/5$. (a) The energy flux densities of $S_{\rm in}$, $S_{\rm up}$, $S_{\rm down}$, and $S_{\rm ab}$. (b) The corresponding emission efficiency ($S_{\rm up}/S_{\rm in}$ and $S_{\rm down}/S_{\rm in}$) and absorption efficiency ($S_{\rm ab}/S_{\rm in}$).

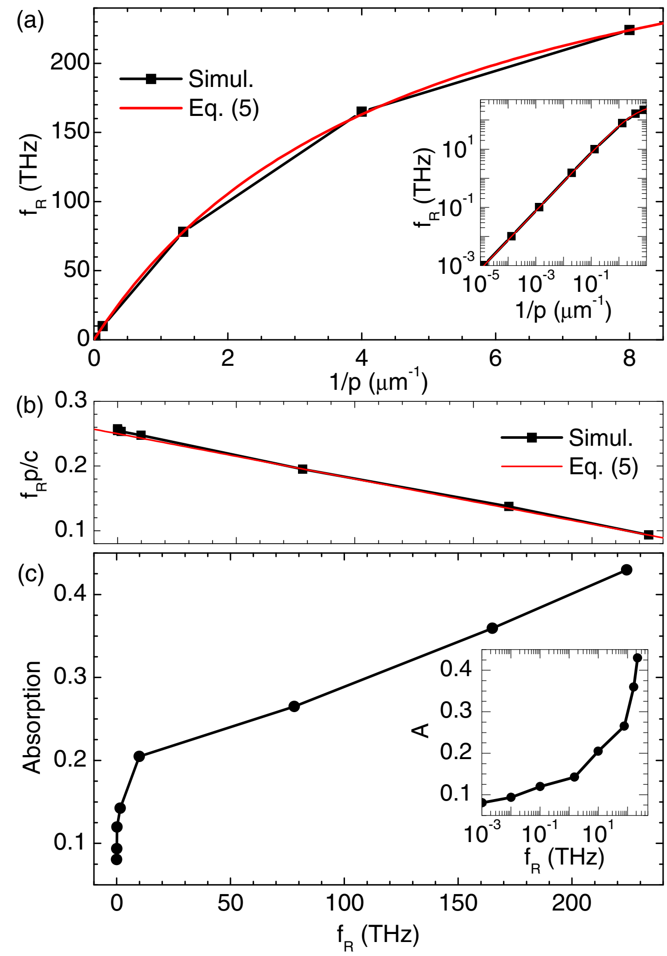

FIG. 4. The behavior of Babinet metasurfaces with different periods p at normal incidence of propagating waves. The metasurfaces have the same parameters as in Fig. 2 but with different periods p. (a) The resonant frequency f_R as a function of $1/p$. (b) pf_R/c and (c) the absorption at f_R as a function of f_R. (a) and (c) are replotted with a logarithmic scale in the insets. $pf_R = v$ in (b) presents the velocity of charged particles in Fig. 5.

However, the emission efficiencies and loss ratio are nearly not changed [38].

The above studies are focused on the Babinet metasurface with period $p = 50$ μm. We then simulate metasurfaces with other periods ($p = 0.125$ μm, 0.25 μm, 0.75 μm, 7.5 μm, 0.75 mm, 7.5 mm, and 75 mm) under normal incidence of propagating waves. The corresponding resonant frequencies, plotted in Fig. 4(a), can be further fitted with a simple formula

$$f_R = v_0/(p + p'), \qquad (5)$$

where $v_0 = 0.25c$ and $p' = 0.21$ μm. For large periods ($p > 10p'$), Eq. (5) reduces to $f_R \approx v_0/p$, so that the resonant frequency is proportional to the reciprocal of period. But for small periods ($p \ll p'$), the resonant frequency is independent on the period and has an upper limit of $f_\infty = v_0/p' = 357.1$ THz. This phenomenon has also been observed in the reverse structure of Babinet metasurfaces (i.e., split-ring resonators), which can be understood by the electron kinetic energy in split-ring resonators for high frequencies [39]. When the period is much smaller than p', split-ring resonators cannot exhibit artificial magnetic response [39].

From Fig. 4(a), the dependence of pf_R/c on f_R can be obtained [see Fig. 4(b)]. The results can also be fitted by an alternative form of Eq. (5), namely $pf_R = v_0 - p'f_R$. We note that $v_R = pf_R = v_0 - p'f_R$ is just the velocity of charged particle for generating the Smith-Purcell emissions at resonant frequency f_R. Hence, the velocity v_R decreases linearly with increasing the resonant frequency. While the velocities v_R is $0.25c$ at $f_R = 1.51$ THz, it can be lowered to $0.093c$ at $f_R = 224$ THz. We note that a low charged-particle velocity corresponds to a low acceleration voltage (2.22 kV for $0.093c$ and 16.8 kV for $0.25c$) and could be beneficial to fabricating a compact free-electron light source [33].

Figure 4(c) shows the absorption at resonant frequencies for the metasurfaces under normal incidence of propagating waves. We can see that the absorption increases with increasing the resonant frequency f_R. At $f_R = 9.9$ THz (224 THz), the absorption is 0.20 (0.43). When the resonant frequency approaches f_∞, the absorption will be close to 0.5.

The Smith-Purcell effects are further studied for Babinet metasurfaces with different periods. From Fig. 5(a), we can see that, as the resonant frequency increases, the input energy flux density $S_{\rm in}$ and emission energy flux densities ($S_{\rm up}$ and $S_{\rm down}$) decrease while absorption energy flux density $S_{\rm ab}$ increases. Similar changes also exist in the emission efficiencies ($S_{\rm up}/S_{\rm in}$ and $S_{\rm down}/S_{\rm in}$) and loss ratio $S_{\rm ab}/S_{in}$ [see

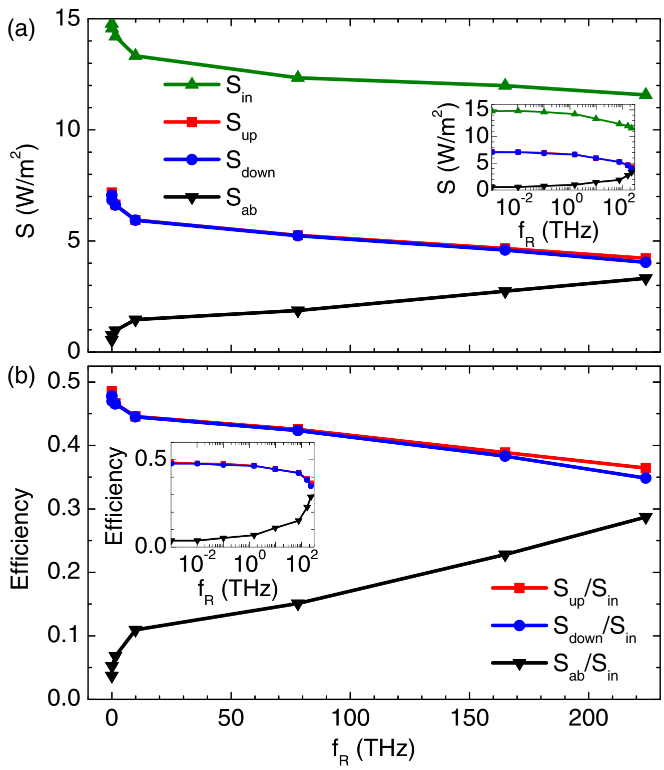

FIG. 5. Characterization of the Smith-Purcell effect from the Babinet metesurfaces with different resonant frequencies f_R. The swift charged particles are described by Eq. (1) with $I_0 = 1$ A/m, $z_0 = p/5$, and $v = pf_R$ [see Fig. 4(b)]. (a) The energy flux densities of $S_{\rm in}$, $S_{\rm up}$, $S_{\rm down}$, and $S_{\rm ab}$. (b) The corresponding emission efficiency ($S_{\rm up}/S_{\rm in}$ and $S_{\rm down}/S_{\rm in}$) and absorption efficiency ($S_{\rm ab}/S_{\rm in}$). (a) and (b) are replotted with a logarithmic scale in the insets.

Fig. 5(c)]. For resonant frequencies lower than 10 GHz, the loss ratio is about 0.037. Although the loss ratio increases with increasing resonant frequency, it remains as low as 0.11 (0.29) at resonant frequency of 10 THz (224 THz). For higher resonant frequencies (approaching f_∞), the loss ratio will be near 0.33 and the total emission ratio $[(S_{\rm up} + S_{\rm down})/S_{\rm in}]$ can be about 0.67.

IV. CONCLUSION

In conclusion, we have demonstrated that Babinet metasurfaces consisting of metallic C-aperture resonators can generate strong Smith-Purcell radiation at resonant frequencies. By adjusting the period of metasurface, the resonant (or working) frequency can be shifted from GHz to THz and infrared ranges. It is found that the absorption loss ratio is 3.7% at a working frequency of 10 GHz. Although the loss ratio increases with increasing the working frequency, it remains as low as 11% (29%) at a working frequency of 10 THz (224 THz). In addition, a nonlinear relationship is found between the resonant frequency and the reciprocal of period, resulting in decreased charged-particle velocity with increasing the working frequency. Our results indicate that Babinet metasurfaces can efficiently generate Smith-Purcell radiation in a wide frequency range. This may benefit the fabrication of compact, efficient THz and infrared light sources.

ACKNOWLEDGMENTS

This work was supported by the 973 Program (Grant No. 2013CB632701) and the National Natural Science Foundation of China (NSFC) (No. 61422504 and No. 11574037).

L.L. and H.C. contributed equally to this work.

[1] S. J. Smith and E. M. Purcell, Phys. Rev. **92**, 1069 (1953).
[2] P. A. Cherenkov, Phys. Rev. **52**, 378 (1937).
[3] J. V. Jelly, *Cerenkov Radiation and Its Applications* (Pergamon, London, 1958).
[4] L. D. Landau, E. M. Liftshitz, and L. P. Pitaevskii, *Electrodynamics of Continuous Media*, 2nd ed. (Pergamon, New York, 1984).
[5] N. Yu and F. Capasso, Nat. Mater. **13**, 139 (2014).
[6] N. Yu, P. Genevet, M. A. Kats, F. Aieta, J. P. Tetienne, F. Capasso, and Z. Gaburro, Science **334**, 333 (2011).
[7] S. L. Sun, Q. He, S. Y. Xiao, Q. Xu, X. Li, and L. Zhou, Nat. Mater. **11**, 426 (2012).
[8] L. L. Huang, X. Z. Chen, H. Muhlenbernd, G. X. Li, B. F. Bai, Q. F. Tan, G. F. Jin, T. Zentgraf, and S. Zhang, Nano Lett. **12**, 5750 (2012).
[9] J. Lin, J. P. B. Mueller, Q. Wang, G. H. Yuan, N. Antoniou, X. C. Yuan, and F. Capasso, Science **340**, 331 (2013).
[10] N. Shitrit, I. Yulevich, E. Maguid, D. Ozeri, D. Veksler, V. Kleiner, and E. Hasman, Science **340**, 724 (2013).
[11] S.-C. Jiang, X. Xiong, Y.-S. Hu, Y.-H. Hu, G.-B. Ma, R.-W. Peng, C. Sun, and M. Wang, Phys. Rev. X **4**, 021026 (2014).
[12] A. Silva, F. Monticone, G. Castaldi, V. Galdi, A. Alù, and N. Engheta, Science **343**, 160 (2014).
[13] J. Lee, M. Tymchenko, C. Argyropoulos, P.-Y. Chen, F. Lu, F. Demmerle, G. Boehm, M.-C. Amann, A. Alù, and M. A. Belkin, Nature (London) **511**, 65 (2014).
[14] F. Aieta, M. A. Kats, P. Genevet, and F. Capasso, Science **347**, 1342 (2015).
[15] M. Pu, X. Li, X. Ma, Y. Wang, Z. Zhao, C. Wang, C. Hu, P. Gao, C. Huang, H. Ren, X. Li, F. Qin, J. Yang, M. Gu, M. Hong, and X. Luo, Sci. Adv. **1**, e1500396 (2015).
[16] X. Ni, Z. J. Wong, M. Mrejen, Y. Wang, and X. Zhang, Science **349**, 1310 (2015).
[17] G. Li, S. Chen, N. Pholchai, B. Reineke, P. W. H. Wong, E. Y. B. Pun, K. W. Cheah, T. Zentgraf, and S. Zhang, Nat. Mater. **14**, 607 (2015).
[18] N. Segal, S. Keren-Zur, N. Hendler, and T. Ellenbogen, Nat. Photon. **9**, 180 (2015).
[19] Z. Wang, K. Yao, M. Chen, H. Chen, and Y. Liu, Phys. Rev. Lett. **117**, 157401 (2016).
[20] J. S. Hummelt, X. Lu, H. Xu, I. Mastovsky, M. A. Shapiro, and R. J. Temkin, Phys. Rev. Lett. **117**, 237701 (2016).
[21] F. J. Garcia de Abajo, Phys. Rev. Lett. **82**, 2776 (1999).

[22] S. Yamaguti, J. I. Inoue, O. Haeberlé, and K. Ohtaka, Phys. Rev. B **66**, 195202 (2002).
[23] C. Luo, M. Ibanescu, S. G. Johnson, and J. Joannopoulos, Science **299**, 368 (2003).
[24] S. Xi, H. Chen, T. Jiang, L. Ran, J. Huangfu, B.-I. Wu, J. A. Kong, and M. Chen, Phys. Rev. Lett. **103**, 194801 (2009).
[25] G. Adamo, K. F. MacDonald, N. I. Zheludev, Y. H. Fu, C. M. Wang, D. P. Tsai, and F. J. Garcia de Abajo, Phys. Rev. Lett. **103**, 113901 (2009).
[26] F. J. Garcia de Abajo, Rev. Mod. Phys. **82**, 209 (2010).
[27] D. E. Fernandes, S. I. Maslovski, and M. G. Silveirinha, Phys. Rev. B **85**, 155107 (2012).
[28] V. V. Vorobev and A. V. Tyukhtin, Phys. Rev. Lett. **108**, 184801 (2012).
[29] S. Liu, P. Zhang, W. Liu, S. Gong, R. Zhong, Y. Zhang, and M. Hu, Phys. Rev. Lett. **109**, 153902 (2012).
[30] T. Zhan, D. Han, X. Hu, X. Liu, S. T. Chui, and J. Zi, Phys. Rev. B **89**, 245434 (2014).
[31] W. Liu and Z. Xu, New J. Phys. **16**, 073006 (2014).
[32] T. Denis, M. W. van Dijk, J. H. H. Lee, R. van der Meer, A. Strooisma, P. J. M. van der Slot, W. L. Vos, and K.-J. Boller, Phys. Rev. A **94**, 053852 (2016).
[33] F. Liu, L. Xiao, Y. Ye, M. Wang, K. Cui, X. Feng, W. Zhang, and Y. Huang, Nat. Photon. **11**, 289 (2017).
[34] M. Tonouchi, Nat. Photon. **1**, 97 (2007).
[35] Q. Guo, C. Zhang, and X. Hu, Sci. Rep. **6**, 32345 (2016).
[36] M. A. Ordal, L. L. Long, R. J. Bell, S. E. Bell, R. R. Bell, R. W. Alexander, Jr., and C. A. Ward, Appl. Opt. **22**, 1099 (1983).
[37] F. Zhao, C. Zhang, H. Chang, and X. Hu, Plasmonics **9**, 1397 (2014).
[38] See Supplemental Material at http://link.aps.org/supplemental/10.1103/PhysRevB.96.165435 for results of Babinet metasurfaces with the orientation of *C* aperture in the *y* direction.
[39] J. Zhou, Th. Koschny, M. Kafesaki, E. N. Economou, J. B. Pendry, and C. M. Soukoulis, Phys. Rev. Lett. **95**, 223902 (2005).